

# Monopolar transcranial direct current stimulation (tDCS) might selectively affect brainstem reflex pathways: a computational and neurophysiological study.

Matteo Guidetti<sup>1</sup>, Anna Bianchi<sup>2</sup>, Marta Parazzini<sup>3</sup>, Natale Maiorana<sup>1</sup>, Marta Bonato<sup>3</sup>, Rosanna Ferrara<sup>1</sup>, Giorgia Libelli<sup>1</sup>, Kora Montemagno<sup>1</sup>, Roberta Ferrucci<sup>1</sup>, Alberto Priori<sup>4</sup>, and Tommaso Bocci<sup>5</sup>

<sup>1</sup>La Statale

<sup>2</sup>Politecnico di Milano

<sup>3</sup>CNR

<sup>4</sup>Universita' di Milano

<sup>5</sup>Universita degli Studi di Milano

March 7, 2023

## Abstract

Non-invasive deep brain stimulation is a novel field of research that aims to affect deep brain regions' activity through non-invasive stimulation. Recent computational and clinical findings have fostered the interest on transcranial direct current stimulation as non-invasive deep brain stimulation techniques, and several optimization strategies have been tested. Multi-electrode transcranial direct current stimulation has shown the potential to selectively affect deep brain structures. Here, we assess whether arbitrarily chosen monopolar multi-electrode transcranial direct current stimulation montages might selectively affect deep brain structures through computational predictions and neurophysiological assessment. Electric field distribution in deep brain structures (i.e., thalamus and midbrain) were estimated through computational models simulating transcranial direct current stimulation with two monopolar and two monopolar multi-electrode montages. Monopolar multi-electrode transcranial direct current stimulation was then applied to healthy subject, and effects on pontine and medullary circuitries was evaluated studying changes in blink reflex and masseter inhibitory reflex. Computational results suggest that transcranial direct current stimulation with monopolar multi-electrode montages might induce electric field intensities in deep brain structure comparable to those in grey matter, while neurophysiological results disclosed that blink reflex and masseter inhibitory reflex were selectively modulated by transcranial direct current stimulation only when cathode was placed over the right deltoid. Therefore, multi-electrode transcranial direct current stimulation (anodes over motor cortices, cathode over right deltoid) could induce significant electric fields in the thalamus and midbrain, and selectively affect brainstem neural circuits. Such strategy should be further explored in the context of non-invasive deep brain stimulation.

## Monopolar transcranial direct current stimulation (tDCS) might selectively affect brainstem reflex pathways: a computational and neurophysiological study.

Matteo Guidetti<sup>1,2</sup>, Anna Maria Bianchi<sup>2</sup>, Marta Parazzini<sup>3</sup>, Natale Maiorana<sup>1</sup>, Marta Bonato<sup>3</sup>, Rosanna Ferrara<sup>1</sup>, Giorgia Libelli<sup>4</sup>, Kora Montemagno<sup>1</sup>, Roberta Ferrucci<sup>1,5</sup>, Alberto Priori<sup>1,5</sup>, Tommaso Bocci<sup>1,5\*</sup>

<sup>1</sup> "Aldo Ravelli" Center for Neurotechnology and Experimental Brain Therapeutics, Department of Health Sciences, University of Milan, Via Antonio di Rudinì 8, 20142 Milan, Italy.

<sup>2</sup> Department of Electronics, Information and Bioengineering, Politecnico di Milano, Piazza Leonardo da Vinci, 32, 20133 Milan, Italy.

<sup>3</sup> Institute of Electronics, Computer and Telecommunication Engineering (IEIIT), CNR, 20133 Milan, Italy.

<sup>4</sup> Neurology Unit, Department of Medicine and Surgery, University of Parma, Via Gramsci 14, 43126, Parma, Italy

<sup>5</sup> Clinical Neurology Unit, "Azienda Socio-Sanitaria Territoriale Santi Paolo E Carlo", Department of Health Sciences, University of Milan, Via Antonio di Rudinì 8, 20142 Milan, Italy

Corresponding author: Dr. Tommaso Bocci, [tommaso.bocci@unimi.it](mailto:tommaso.bocci@unimi.it)

**Running title:** Brainstem stimulation by tDCS

## Acknowledgments

This research did not receive any specific grant from funding agencies in the public, commercial, or not-for-profit sectors

## Abstract

Non-invasive deep brain stimulation is a novel field of research that aims to affect deep brain regions' activity through non-invasive stimulation. Recent computational and clinical findings have fostered the interest on transcranial direct current stimulation as non-invasive deep brain stimulation techniques, and several optimization strategies have been tested. Multi-electrode transcranial direct current stimulation has shown the potential to selectively affect deep brain structures. Here, we assess whether arbitrarily chosen monopolar multi-electrode transcranial direct current stimulation montages might selectively affect deep brain structures through computational predictions and neurophysiological assessment. Electric field distribution in deep brain structures (i.e., thalamus and midbrain) were estimated through computational models simulating transcranial direct current stimulation with two monopolar and two monopolar multi-electrode montages. Monopolar multi-electrode transcranial direct current stimulation was then applied to healthy subject, and effects on pontine and medullary circuitries was evaluated studying changes in blink reflex and masseter inhibitory reflex. Computational results suggest that transcranial direct current stimulation with monopolar multi-electrode montages might induce electric field intensities in deep brain structure comparable to those in grey matter, while neurophysiological results disclosed that blink reflex and masseter inhibitory reflex were selectively modulated by transcranial direct current stimulation only when cathode was placed over the right deltoid. Therefore, multi-electrode transcranial direct current stimulation (anodes over motor cortices, cathode over right deltoid) could induce significant electric fields in the thalamus and midbrain, and selectively affect brainstem neural circuits. Such strategy should be further explored in the context of non-invasive deep brain stimulation.

**Keywords:** Neuromodulation, Transcranial Direct Current Stimulation, Computational Model, Blink Reflex, Masseter Inhibitory Reflex, Non-Invasive Deep Brain Stimulation

## Introduction

Transcranial direct current stimulation (tDCS) is a non-invasive brain stimulation (NIBS) technique which has gained great interest in recent years, due to its safety (Antal et al., 2017), feasibility (Siebner et al., 2004; Woods et al., 2016), affordability (Evidence-based guidelines on the therapeutic use of transcranial direct current stimulation (tDCS), 2017; Manto et al., 2021), and available clinical evidences (for a review, see (Evidence-based guidelines on the therapeutic use of transcranial direct current stimulation (tDCS), 2017)). Low-amplitude (typically 1-2 mA) direct current is injected in the brain via scalp electrodes, and generates small electrical fields (EF) responsible of biological (Guidetti, Bertini, et al., 2022) and, ultimately, behavioural changes (D'Urso et al., 2015; Ferrucci et al., 2009; Peterchev et al., 2012), together with the individual anatomy (Opitz et al., 2015). Computational models (Gomez-Tames et al., 2020; Parazzini et al., 2011, 2012; Rashed et al., 2020; Thomas et al., 2019) and in vivo recordings (Guidetti, Arlotti, et al., 2022) reported that tDCS can generate significant EF in subcortical regions, possibly modifying their activity. However, stimulation in depth is not focal (Huang & Parra, 2019) and tDCS-induced EF is hardly controllable (Datta et al., 2009). EF necessarily passes through superficial areas, spreading over non-cerebral zones

because of the dispersion in the tissues (Opitz et al., 2015) and the high conductivity of cerebrospinal fluid (Opitz et al., 2015). Also, EF decays in intensity and focality with increasing depth (Bikson & Dmochowski, 2020). Physically, the distribution of the EF depends upon the temporal (e.g., waveform) and spatial (e.g., electrodes’ position) characteristics of the current injected (Peterchev et al., 2012). Therefore, several authors have tried to steer the EF by modifying these parameters of the stimulation, and proposing different strategies (Grossman et al., 2017; Huang et al., 2020; Huang & Parra, 2019). For example, by setting number and position of scalp electrodes – a strategy called multi-electrode tDCS (Optimized multi-electrode stimulation increases focality and intensity at target, 2011; Guler et al., 2016; Ruffini et al., 2014; Sadleir et al., 2012; Wagner et al., 2016), which might be able to direct the current toward or away from specific brain areas (Sadleir et al., 2012). Also, it would induce more focalized (Park et al., 2011; Ruffini et al., 2014; Wagner et al., 2016) and intense (Khorrampanah et al., 2020; Wagner et al., 2016) stimulation at brain cortical targets (Khan et al., 2022; Park et al., 2011). Sadleir et al. (2012) successfully demonstrated that optimized multi-electrode montages could not only steer current in deep brain structures (namely, nuclei accumbens), but also avoid the left inferior frontal gyrus while targeting basal ganglia, and vice versa (Sadleir et al., 2012). Huang et al. (2019) (Huang & Parra, 2019) computationally demonstrated that tDCS applied with an appropriate multi-electrode montages can induce significant stimulation in deep targets, with cerebrospinal fluid directing currents deep into the brain. Taken together, these findings have fostered the interest in tDCS as a non-invasive deep brain stimulation (NDBS) technique (Huang & Parra, 2019), a new field of research that aims to affect deep brain regions’ activity through NIBS methods (Bikson & Dmochowski, 2020). NDBS would allow to directly target those anatomical deep substrates mainly involved in neurological pathologies (e.g., subthalamic nucleus in Parkinson’s disease) (Gunalan et al., 2018) without resorting to neurosurgery as in other neurostimulation techniques (Marceglia et al., 2021; Priori et al., 2021).

Here, we investigate the ability of a series of tDCS montages to steer the EF in deep brain structures by applying the multi-electrode approach. We arbitrarily considered extracephalic montages, i.e., placing two anodes over the scalp and one cathode far from the scalp (namely, over the right deltoid and over the 10<sup>th</sup> thoracic vertebra). Indeed, several studies suggest that the extracephalic reference induces a concentration of currents (Mendonca et al., 2011; Noetscher et al., 2014) and greater EF in deeper brain structures (e.g., cerebellum, thalamus and striatum midbrain, pons and medulla) compared to cephalic montages (Bai et al., 2014; Parazzini et al., 2013). We aimed to:

Estimate the EF in 4 regions of interest (ROIs - grey matter, hippocampus, thalamus and mid-brain) as modelled in an MRI-based realistic human head model (Christ et al., 2010).

Validate the estimates in deep brain structures by analysing electrophysiological responses (blink reflex – BR, and masseter inhibitory reflex - MIR) reflecting the activity of pontine and low medullary neuronal circuitries. The neurophysiological study is thought to extend our computational data, as it refers to anatomical structures deeper than those analysed by MRI-based human models.

## Materials e methods

### High-Resolution Computational Model

In the computational study, the quasi-static Laplace equation was solved by the simulation platform Sim4life (from ZMT Zurich Med Tech AG, Zurich, Switzerland, [www.zurichmedtech.com](http://www.zurichmedtech.com)) to determine the tDCS-induced electric potential ( ) distribution in human head tissue:

$$\nabla \cdot (\sigma \nabla \phi) = 0$$

where  $\sigma$  is the electrical conductivity of the human tissues. The distribution of EF was obtained by means of the equations:

$$EF = -\nabla \phi$$

A finite element method (FEM) realistic human model based on high-resolution magnetic resonance images of healthy volunteers (Christ et al., 2010) was used. The human model “Ella” (a 26-year-old female adult)

consisted of 76 different tissues with dielectric properties assigned according to literature data (Gabriel et al., 1996, 2009).

We modelled the electrodes in the following positions, according to the 10–20 system, as previously explored (Cogiamanian et al., 2007; Fertoni et al., 2010; Mesquita et al., 2020; Parazzini et al., 2013) (see fig. 1):

- I) Montage A1: active electrode over the vertex, return electrode over right deltoid.
- II) Montage A2: active electrode over C3 and C4, return electrode over right deltoid.
- III) Montage B1: active electrode over the vertex, return electrode over the spinal process of the 10<sup>th</sup> thoracic vertebra.
- IV) Montage B2: active electrode over C3 and C4, return electrode over the spinal process of the tenth thoracic vertebra.

For comparative purposes, we considered a fifth cephalic montage (Montage C), i.e., active electrode over left M1 (C3) and return electrode over the right supraorbital region (Fp2). Electrodes were modelled as a rectangular pad conductor (5x5 cm,  $\sigma = 5.9 \times 10^7$  S/m) with a thickness of 1 mm. Their lower surface is separated from the skin by a layer of 5 mm of conductive gel ( $\sigma = 1.4$  S/m), shaped as the conductor itself. In each computational simulation, the upper surface of each electrode was set to a uniform electrical potential and the potential difference between the electrodes was adjusted so that the current injected through the anode(s) was the desired value (2 mA).

For each simulation, the model (i.e., human model plus electrodes) was placed in a surrounding bounding box filled with air and the model was trunked at the pelvis level for electrode montages A1-B2 and at the shoulder level for the electrode montage C. The boundaries of the bounding box were treated as insulated except the truncation section of the Ella model, which was assigned with a boundary condition of continuity of the current. Continuity of the tangential component of EF was applied at each tissue-to-tissue boundary. At the interface between the skin and the air, the current density was set to be parallel to the surface.

The computational domain was discretized by uniform rectilinear grid, with a mesh step equal to 1 mm to allow a good discretization of the anatomical model.

For each montage model, the amplitude of EF was computed and analysed in 4 different ROIs: grey matter (GM), hippocampus (HPC), mid-brain (MB), and thalamus (THA) (see fig.2, first row). For each EF distribution, we estimated the “peak” (i.e., the 99th percentile), the median amplitude, the 25<sup>th</sup> and 75<sup>th</sup> percentile. Furthermore, we estimated the percentage of area of hippocampus, mid-brain, and thalamus where the amplitude of EF was greater than 25% (V25), 30% (V30), and 50% (V50) of 99th percentile in grey matter. All these values have been calculated as normalized to the 99<sup>th</sup> percentile of E in the grey matter for each montage.

## Neurophysiological study

### Subjects

The experimental study was conducted on ten healthy volunteers (mean  $\pm$  SD age:  $31.5 \pm 9.7$ , 5 women). The exclusion criteria were as follows: 1) age  $< 18$  years; 2) history and/or current signs or symptoms of major neurologic, neuropsychological, and psychiatric diseases, as excluded by clinical history and anamnestic interview; 3) pregnancy; 4) presence of a pacemaker, intracranial metal, or spinal cord stimulators; 5) history and/or current signs or symptoms of dental pathologies and/or surgery involving the alveolar branch of the mental nerve. The study protocol followed the Declaration of Helsinki and was approved by the Ethics Committee of the ASST Santi Paolo e Carlo - Hospital of Milan. All subjects gave written informed consents before the participation.

### Study protocol

In this experimental, assessor-blinded, randomized crossover study, each volunteer underwent bilateral motor anodal tDCS (2mA for 20 min) with cathode over right deltoid (condition E1) and over T10 (condition E2) in two different sessions separated by a washout period of at least 1 week to avoid possible carryover effect. A

further control condition was considered (condition Ec – 1.75mA for 20min), where anode was placed over left motor cortex, and cathode over contralateral supraorbital region (see fig.3). The order of the experimental conditions was randomized across the subjects (see fig.4). BR and MIR were recorded immediately before (T0) and after (T1) the stimulations.

### **tDCS experimental protocol**

DC stimulation was applied by a stimulator (HDCStim, Newronika, Italy) connected to silicone rubber pad electrodes with thickness of 1 mm and an area of 35 cm<sup>2</sup> (7 × 5 cm<sup>2</sup>) for the anodes, 48 cm<sup>2</sup> (8 x 6 cm<sup>2</sup>) for the cathode. Conductive gel was applied between the electrodes and the skin to reduce and stabilize contact impedance during stimulation. We clinically replicated the multi-electrode montages that predicted the highest intensities of EF in MB and THA, as shown in the previous computational study. We chose Montage A2 and Montage B2 because the EF amplitudes in deep regions were comparable to those in grey matter, with higher values compared to the other Montages tested. Therefore, anodes were applied bilaterally over the motor cortex (C3 and C4 scalp positions of the International EEG 10/20 system), while cathodes were placed over left deltoid (condition E1) or over T10 (condition E2). As control condition, a third montage (anode over C3, cathode over Fp2) was considered (condition Ec). DC was applied at 2mA for E1, E2 conditions, and 1.75 mA for Ec condition, to keep the current density (current strength divided by electrode size) constant in all the conditions (current density = 0.028 mA/cm<sup>2</sup>) for 20 min with a 30s ramp-up before tDCS and 30 s ramp-down after tDCS. We considered values of current density way lower than limits commonly accepted (Bikson et al., 2009).

### **Blink Reflex (BR) recording**

Two of the investigators, who were blinded to the stimulation setting, performed the evaluation, and took the measurements. During the assessments, participants were sitting in a comfortable chair and instructed to keep their eyes open and fix a target placed 1 m in front of them. The right and left supraorbital nerve were consecutively stimulated through a pair of silver chloride cup electrodes (cathode over the supraorbital foramen; anode 2 cm above). A constant current with pulse width 200 µs and inter-trial interval ranging between 25 and 35 s to avoid habituation was used as stimulation (Aramideh & Ongerboer De Visser, 2002; Esteban, 1999). The stimulation point, at both sides, was marked with a pencil in order to ensure reproducibility between different assessment sessions (T0 and T1). EMG activity was bilaterally recorded from the orbicularis oculi muscle, via surface electrodes (active electrode over the mid-lower eyelid; reference electrode laterally to the lateral canthus). A total of 8 responses was recorded on each side. Electromyographic signal (band-pass 10 Hz–10 kHz, sampling rate 20 kHz, sensitivity set 500 µV/Div; sweep speed 10 ms/Div) was collected from superimposed traces and stored for offline analysis. Recording electrodes were kept in the same position on the skin during tDCS. The reflex Threshold (mV), as well as latencies (ms) of the two main components, formally named RI and RII (ipsilateral and contralateral), was considered for statistical analysis (see fig. 5). These two responses originate from different pathways, at a low-pontine and medullary level respectively (Bocci et al., 2021; Esteban, 1999).

### **Masseter Inhibitory Reflex (MIR) recording**

Two of the investigators, who were blinded to the stimulation setting, performed the evaluation, and took the measurements. The method of recording the masseter inhibitory reflex is reported in details elsewhere (Schoenen, 1993). Briefly, subjects were asked to clench their teeth as strong as possible, as confirmed by audio-visual examination of electromyographic activity. Sweep speed was set at 50 ms per division and band-pass filters at 20 HZ to 10 kHz. EMG signals were recorded through surface electrodes from the masseter muscles bilaterally, with the active electrode placed over the lower third of the muscle belly and the reference approximately 2 cm below the mandibular angle (Crucchi & Deuschl, 2000; Kennelly, 2019). Recording electrodes were kept in the same position on the skin during tDCS. Then, the inferior alveolar branch of the mental nerve was stimulated transcutaneously with the cathode positioned over the mental foramen and the anode placed 1 cm laterally. An electrical square-wave pulse (0.1 ms duration) was delivered, and the stimulus intensity set at 2.5 times the reflex threshold (range 15–45 mA, approximately 8-10 times

the sensory threshold). The stimulation point was marked with a pencil to ensure reproducibility between different assessment sessions (T0 and T1). The lingual nerve was not stimulated, as this alternative procedure for MIR recording is usually devoted to the assessment of iatrogenic damage after third molar extraction. Eight traces were recorded for each side and signals superimposed for off-line analyses. Both onset latencies and duration of the two Silent Periods (formally named SP1 and SP2) was considered for statistical analysis (see fig. 6). These periods are mediated by non-nociceptive A-beta afferents through oligosynaptic (SP1) and polysynaptic (SP2) circuits, partly overlapping with those involved in BR generation, with a slightly more dorsal and lateral localization regarding SP2 as compared to RII (Cruccu et al., 1989, 2005).

## Statistical Analysis

Normal distributions of the dependent variables were assessed via Shapiro-Wilk Test for normality, which is the more appropriate method for small sample sizes (Mishra et al., 2019). All data sets passed the test ( $p > 0.05$ ), therefore parametric analysis was considered. Paired t-Test (T0 vs T1) was used to assess the effect of each treatment (condition E1, condition E2, condition Ec) on neurophysiological variables. In all the analysis, a p-value  $< 0.05$  was set as significant. The data were analysed using JASP v. 0.16.3 for Windows (JASP Team, 2022).

## Results

### Electric field estimations

Fig. 7 shows the amplitude of EF in the HPC, MB, and THA for the five electrode montages, as normalized to the 99th percentile of EF in the grey matter for each montage. For each montage, medians, 25<sup>th</sup> and 75<sup>th</sup> percentiles in deeper regions are roughly comparable to those in the grey matter when the return electrode is extracerebral, with peak values always above 65% of the peak in the grey matter (Fig. 7 - A1, A2, B1 and B2). However, montage A2 and B2 (i.e., multi-electrode montages with 2 active electrodes over the skull) resulted in higher normalized 25<sup>th</sup> percentiles, medians, and 75<sup>th</sup> percentiles in deeper brain structures. Conversely, values of EF in montage C are remarkably lower compared to the other montages considered for all the ROIs, with peaks always lower than 33% of the peak in the grey matter (Fig. 7 - C). Fig. 2 (second and third row) shows the graphical views of the amplitude distribution of EF in GM, HPC, MB, and THA for Montage A2 and B2. We chose to show only these montages' graphical outcomes because they predicted the highest intensities of EF in deep structures and were chosen for clinical applications. As for the volume percentage, Fig. 8 shows the V25s, V30s and V50s of HPC, MB, and THA for the five electrode montages, as normalized to the 99th percentile of EF in the grey matter for each montage. Montages with return electrode over the shoulder (Montage A1, Montage A2) and the spine (Montage B1, Montage B2) had values one order of magnitude greater than those in Montage C, with values of V50 one hundred times higher. Montages A1 and B1 showed a similar pattern of percentages, with close V25, V30 and V50 (Fig.8). Montage A2 and B2 resulted in similar volumes for each structure as well, but with remarkably higher values both for V25, V30 and V50 compared to A1 and B1 montages (Fig.8).

### Neurophysiological outcomes

No significant changes in neurophysiological variables over time were disclosed for condition E2 and condition Ec (for all the analysis,  $p > 0.05$ , paired sample T-Test), but a significant reduction in latency of RI [right BR:  $t(9) = 5.24$ ,  $p < 0.001$ ; left BR:  $t(9) = 3.21$ ,  $p = 0.01$ ] and increase of SP1 duration of MIR [ $t(9) = -2.46$ ,  $p = 0.03$ ] in condition E1 (Table 1; fig.9). Also, a tendency to increase the values RII latency – ipsilateral and contralateral for right BR – was found (respectively,  $p = 0.052$  and  $p = 0.054$ ) after condition E1 (Table 1; fig.9).

## Discussion and Conclusions

In this study, we computationally estimated the trends of EF distributions in 4 ROIs (GM, HPC, MB and THA) during multielectrode tDCS with extracerebral reference, and clinically tested their effects on trigemino-facial reflexes (BR and MIR). Our results suggest that extracerebral montages might induce a

deeper and more focal distribution of EF compared to control cephalic montage, as suggested by the values in deep structures and the volumes of THA and MB virtually modulated. Also, clinical findings seem to confirm that bilateral motor anodal tDCS with extracephalic cathode (over right deltoid, but not over T10) induces changes in BR and MIR, whereas control cephalic montage leaves these parameters unchanged.

Several computational studies have suggested that setting number and position of scalp electrodes during tDCS could help in increasing the intensity and focality of stimulation in a target zone (D'Urso et al., 2022; Khorrampanah et al., 2020; Wagner et al., 2016). For example, Khorrampanah et al., 2020 (Khorrampanah et al., 2020) demonstrated that arbitrarily chosen multi-electrode montages could be optimized to induce a maximum EF distribution in targeted region which was higher compared to High-definition tDCS (HD-tDCS), also at the inner layers of the head. It is worth pointing out that HD-tDCS is a technically enhanced version of tDCS, which is believed to be more focal (Kuo et al., 2013). Also, some authors proposed that the same results might be optimized for deep brain targets (Optimized Transcutaneous Spinal Cord Direct Current Stimulation using Multiple Electrodes from 3/9/7 System, 2019; Sadleir et al., 2012). However, none of these studies were clinically confirmed, nor considered to use an extracephalic electrode (namely, the cathode - classically, placed over right deltoid or the spine (Bikson et al., 2019)). Indeed, the position of the return electrode, for a fixed position of active electrode, affects the tDCS-induced current distribution and brain modulation (Mendonca et al., 2011; Nitsche & Paulus, 2000; Priori et al., 1998). Although little is known about the actual current passing through the brainstem and other subcortical nuclei when an extracephalic cathode is used (Im et al., 2012; Parazzini et al., 2013, 2014), several studies have investigated such issue (Bai et al., 2014; Im et al., 2012; Mendonca et al., 2011; Noetscher et al., 2014; Parazzini et al., 2013). It has been computationally suggested that moving the cathode outside the scalp induces a concentration of currents (Mendonca et al., 2011; Noetscher et al., 2014). When compared to cephalic configurations, extracephalic montages induced significant amount of current under the active electrode, rather than between the electrodes (Mendonca et al., 2011; Noetscher et al., 2014). Although these results are still matter of debate (Im et al., 2012), we observed that in Ec condition (i.e., cephalic configuration), V25 and V30 were more than 10 times, and V50 more than 100 times, lower compared to other extracephalic montages (A1, A2, B1 and B2). This observation suggests that extracephalic configurations could induce a focalisation of electric modulation. Also, our results showed that trends of EF in THA and MB were comparable to those in the GM for extracephalic montages, suggesting that they might result in substantially greater depth of stimulation compared to C3-Fp2 configuration. Although the assumption is still controversial (Im et al., 2012), several models in literature confirm our predictions (Bai et al., 2014; Noetscher et al., 2014; Parazzini et al., 2013). For example, for fixed anode placement (over left frontal cortex), cathode over the right deltoid developed an EF in the cerebellum, deep central structures (THA, striatum) and brainstem, greater than those developed with cathode over contralateral supraorbital region (Bai et al., 2014). Since neurons in deep brain regions are directly sensitive to weak electric fields (Francis et al., 2003; Reato et al., 2010) and to DC stimulation (Bikson et al., 2004; Chakraborty et al., 2018; Kronberg et al., 2020), an effect similar to those induced by tDCS at cortical level might be expected.

Our neurophysiological findings might confirm computational predictions, but only for E1 condition. Bimotor anodal tDCS with cathode over right deltoid reduced latency of RI in right and left BR, and increased SP1 duration of MIR, suggesting a neuromodulatory effect on brainstem. Indeed, both BR and MIR arcs relies on brainstem neural circuits, which integrate afferent limb (respectively, ophthalmic division of the trigeminal nerve and mental branch of the trigeminal nerve) with efferent limb (respectively, facial nerve and mandibular branch of the trigeminal nerve) (Aramideh & Ongerboer De Visser, 2002; Cosentino et al., 2022; Cruccu et al., 1990; Kugelberg, 1952). In details, for BR, afferent stimuli elicit two responses, RI and RII. For RI response, the sensory stimulus is conducted through the pons, relayed in the vicinity of the main sensory nucleus of the trigeminal nerve (Kimura, 1975; Shahani & Young, 1972), and, finally, reaches the ipsilateral facial nucleus in the lower pontine tegmentum (Esteban, 1999). For ipsilateral RII, the afferent impulse is conducted through the descending spinal tract of the trigeminal nerve in the pons and medulla oblongata, relayed in the caudal spinal trigeminal nucleus by a medullary pathway (Kimura & Lyon, 1972; Ongerboer De Visser & Kuypers, 1978), and ascends bilaterally to reach the facial nuclei in the pons thus inducing contralateral RII responses

(Holstege et al., 1986; Ongerboer De Visser & Kuypers, 1978). For MIR, after stimulation, the impulse reaches the pons through the sensory mandibular root of the trigeminal nerve (Ongerboer De Visser & Goor, 1976). In the ipsilateral trigeminal motor nucleus, an inhibitory interneuron projects onto jaw-closing motoneurons bilaterally, inducing SP1 response (De Visser et al., 1990). As for SP2 response, stimulus is conducted to the lateral reticular formation, where an inhibitory interneuron conducts it to ipsilateral and contralateral trigeminal motoneurons (De Visser et al., 1990). In order to integrate computational data with the neurophysiological outcome, we can hypothesize that tDCS may interfere with diencephalic nuclei strictly connected to pontine and medullary areas from which BR and MIR originate; in particular, a cholinergic downstream has been recently identified between the hypothalamic paraventricular nucleus and different brainstem nuclei (comprising reticular formation, locus ceruleus, dorsal raphe nucleus and motor nucleus of the vagus) (Fearon et al., 2021). However, BR parameters might be influenced by structures above the brainstem, e.g., motor cortex and basal ganglia (Esteban, 1999). Computational studies report, also for multi-electrode tDCS, that it is not possible to avoid delivering current to peripheral cortical regions while targeting deep structures (Sadleir et al., 2012; Wagner et al., 2016). In 2016, Cabib et al. (Cabib et al., 2016) found that biemispheric (anode-C3, cathode-C4) and uniemispheric (anode-C3, cathode-Fp3) tDCS significantly changed BR excitability, and explained this result with a tDCS-induced supranuclear activation conveyed via cortico-reticular (Nonnekes et al., 2014) or cortico-nuclear connections (Berardelli et al., 1983; Fisher et al., 1979; Kuypers, 1958). Also, both BR and MIR arc rely on trigeminal nerve, which is constantly activated during tDCS as suggested by the fact that almost all subjects report different types of sensations under the electrodes (i.e., in the sensory territory of trigeminal nerve) (*Transcranial direct current stimulation: State of the art 2008*, 2008). The continuous sensory inputs via trigeminal afferents on brainstem interneurons may sensitize reflex circuits (Bologna et al., 2010; Manca et al., 2001; Mao & Evinger, 2001) and lead to the enhancement of reflex excitability (Cabib et al., 2016).

In our study, we performed a control stimulation condition (Ec) to exclude that activation of descending cortical pathways and/or sensitization of trigeminal nerve could confound the results. Indeed, control montage had electrodes on both left and right trigeminal territory of innervation, and the anode was placed over left motor cortex. Although this montage was slightly different than previous study (Cabib et al., 2016), still significant changes in BR and MIR were found only for E1 stimulation. This might suggest a frank effect of stimulation. Furthermore, we found changes only in RI latency, which is reported to be resistant to suprasegmental, supratentorial, and cognitive influences (Cruccu & Deuschl, 2000), and in SP1 duration, which is topodiagnostically equivalent to RI (Cruccu et al., 2005). We found no evidence of changes in RII, which is reported to be strongly susceptible to suprasegmental, cortical and cognitive influences (Kimura et al., 1994). Cortical influences for RII generation are confirmed by data showing that NIBS applied over the primary motor cortex are able to modulate RII recovery cycle only, without significant after-effects on RI amplitudes and latencies (De Vito et al., 2009). Moreover, in order to avoid cortical influences possibly underlying our results, it should be considered that differences in tDCS montages, as well as electrodes size and number, impact intracortical excitability in a similar extent, as assessed by Short Intracortical Inhibition (SICI), Intracortical Facilitation (ICF) and Short Intracortical facilitation (SICF) (Pellegrini et al., 2021).

The present work has some limitations. As for the computational models, the results were obtained without accounting for interindividual variability which may influence EF magnitude and spatial distribution (Datta et al., 2010), and montages to be tested were arbitrarily chosen and not optimized. Also, the model used only comprised of a limited number of tissues, potentially arising errors from the exclusion of the dielectric properties of other tissues. As for the clinic study, larger population should be tested for confirmations, and investigations targeting neuronal excitability (e.g., TMS studies (Roos et al., 2021) or studies assessing trigeminal pathways through paired stimulation (KIMURA, 1973)) should be performed to better elucidate the real effect of stimulation on brainstem circuitry. Finally, as shown for other forms of stimulation (Lamy & Boakye, 2013), both the polarity and depth of tDCS after-effects are likely influenced by genetic polymorphisms (Fritsch et al., 2010; Lamy & Boakye, 2013), as well as by the pre-existing excitability state of either cortical or subcortical structures (Bocci et al., 2014; Lang et al., 2007; Siebner et al., 2004).

In conclusion, our computational and clinical results suggest that multi-electrode tDCS considering two



anodes over the motor cortices and the cathode over the right deltoid muscle might induce selective activation of brainstem neuronal circuits. However, given the complexity of brain targeting, future studies might resort to optimization decisional algorithms to achieve an efficient trade-off between intensity, focality, and directionality (Khan et al., 2022). Also, given the importance of inter-subject variability, individualized multi-electrode tDCS should be considered (Khan et al., 2022).

### Conflict of Interest Statement

M.G., A.M.B., M.P., N.M., M.B., Ros.F., G.L., K.M. and T.B. declare no conflict of interest. R.F. and A.P. are founders and shareholders of Newronika Spa.

### Data availability statement

Data are available from the corresponding author on request

### Author contributions

**Matteo Guidetti** : Conceptualization; Data curation; Formal analysis; Investigation; Methodology; Writing - original draft; Writing - review & editing. **Anna Maria Bianchi** : Conceptualization; Supervision; Validation; Visualization; Writing - review & editing. **Marta Parazzini** : Conceptualization; Supervision; Validation; Visualization; Writing - review & editing. **Natale Maiorana** : Investigation; Methodology; Writing - review & editing. **Marta Bonato** : Investigation; Methodology; Writing - review & editing. **Rosanna Ferrara** : Investigation; Writing - review & editing. **Giorgia Libelli** : Investigation; Writing - review & editing. **Kora Montemagno** : Investigation; Writing - review & editing. **Roberta Ferrucci** : Supervision; Validation; Writing - review & editing. **Alberto Priori** : Conceptualization; Data curation; Formal analysis; Methodology; Supervision; Validation; Writing - review & editing. **Tommaso Bocci** : Conceptualization; Data curation; Formal analysis; Investigation; Methodology; Supervision; Validation; Visualization; Writing - original draft; Writing - review & editing.

### Ethical Statement

The study protocol followed the Declaration of Helsinki and was approved by the Ethics Committee of the ASST Santi Paolo e Carlo - Hospital of Milan. All subjects gave written informed consents before the participation.

### Reference

- Antal, A., Alekseichuk, I., Bikson, M., Brockmüller, J., Brunoni, A. R., Chen, R., Cohen, L. G., Douthwaite, G., Ellrich, J., Flöel, A., Fregni, F., George, M. S., Hamilton, R., Haueisen, J., Herrmann, C. S., Hummel, F. C., Lefaucheur, J. P., Liebetanz, D., Loo, C. K., ... Paulus, W. (2017). Low intensity transcranial electric stimulation: Safety, ethical, legal regulatory and application guidelines. In *Clinical Neurophysiology* (Vol. 128, Fascicolo 9, pp. 1774–1809). Elsevier Ireland Ltd. <https://doi.org/10.1016/j.clinph.2017.06.001>
- Aramideh, M., & Ongerboer De Visser, B. W. (2002). Brainstem reflexes: Electrodiagnostic techniques, physiology, normative data, and clinical applications. *Muscle and Nerve* , 26 (1), 14–30. <https://doi.org/10.1002/MUS.10120>
- Bai, S., Dokos, S., Ho, K. A., & Loo, C. (2014). A computational modelling study of transcranial direct current stimulation montages used in depression. *NeuroImage* , 87 , 332–344. <https://doi.org/10.1016/J.NEUROIMAGE.2013.11.015>
- Berardelli, A., Accornero, N., Cruccu, G., Fabiano, F., Guerrisi, V., & Manfredi, M. (1983). The orbicularis oculi response after hemispherical damage. *Journal of Neurology, Neurosurgery & Psychiatry* ,46 (9), 837–843. <https://doi.org/10.1136/JNNP.46.9.837>
- Bikson, M., Datta, A., & Elwassif, M. (2009). Establishing safety limits for transcranial direct current stimulation. *Clinical neurophysiology : official journal of the International Federation of Clinical Neurophysiology* , 120 (6), 1033. <https://doi.org/10.1016/J.CLINPH.2009.03.018>

- Bikson, M., & Dmochowski, J. (2020). What it means to go deep with non-invasive brain stimulation. In *Clinical Neurophysiology* (Vol. 131, Fascicolo 3, pp. 752–754). Elsevier Ireland Ltd. <https://doi.org/10.1016/j.clinph.2019.12.003>
- Bikson, M., Esmaeilpour, Z., Adair, D., Kronberg, G., Tyler, W. J., Antal, A., Datta, A., Sabel, B. A., Nitsche, M. A., Loo, C., Edwards, D., Ekhtiari, H., Knotkova, H., Woods, A. J., Hampstead, B. M., Badran, B. W., & Peterchev, A. V. (2019). Transcranial electrical stimulation nomenclature. *Brain Stimulation* , 12 (6), 1349–1366. <https://doi.org/10.1016/j.brs.2019.07.010>
- Bikson, M., Inoue, M., Akiyama, H., Deans, J. K., Fox, J. E., Miyakawa, H., & Jefferys, J. G. R. (2004). Effect of uniform extracellular DC electric fields on excitability in rat hippocampal slices in vitro. *Journal of Physiology* , 557 (1), 175–190. <https://doi.org/10.1113/jphysiol.2003.055772>
- Bocci, T., Bulfamante, G., Campiglio, L., Coppola, S., Falleni, M., Chiumello, D., & Priori, A. (2021). Brainstem clinical and neurophysiological involvement in COVID-19. *Journal of Neurology* , 268 (10), 3598–3600. <https://doi.org/10.1007/s00415-021-10474-0>
- Bocci, T., Caleo, M., Tognazzi, S., Francini, N., Briscese, L., Maffei, L., Rossi, S., Priori, A., & Sartucci, F. (2014). Evidence for metaplasticity in the human visual cortex. *Journal of Neural Transmission* , 121 (3), 221–231. <https://doi.org/10.1007/S00702-013-1104-Z/FIGURES/4>
- Bologna, M., Agostino, R., Gregori, B., Belvisi, D., Manfredi, M., & Berardelli, A. (2010). Metaplasticity of the human trigeminal blink reflex. *European Journal of Neuroscience* , 32 (10), 1707–1714. <https://doi.org/10.1111/J.1460-9568.2010.07446.X>
- Cabib, C., Cipullo, F., Morales, M., & Valls-Sole, J. (2016). Transcranial Direct Current Stimulation (tDCS) Enhances the Excitability of Trigemino-Facial Reflex Circuits. *Brain Stimulation* , 9 (2), 218–224. <https://doi.org/10.1016/J.BRS.2015.12.003>
- Chakraborty, D., Truong, D. Q., Bikson, M., & Kaphzan, H. (2018). No Title. *Cerebral Cortex* , 28 (8), 2786–2794.
- Christ, A., Kainz, W., Hahn, E. G., Honegger, K., Zefferer, M., Neufeld, E., Rascher, W., Janka, R., Bautz, W., Chen, J., Kiefer, B., Schmitt, P., Hollenbach, H. P., Shen, J., Oberle, M., Szczerba, D., Kam, A., Guag, J. W., & Kuster, N. (2010). The Virtual Family—Development of surface-based anatomical models of two adults and two children for dosimetric simulations. *Physics in Medicine and Biology* , 55 (2), 23. <https://doi.org/10.1088/0031-9155/55/2/N01>
- Cogiamanian, F., Marceglia, S., Ardolino, G., Barbieri, S., & Priori, A. (2007). Improved isometric force endurance after transcranial direct current stimulation over the human motor cortical areas. *European Journal of Neuroscience* , 26 (1), 242–249. <https://doi.org/10.1111/J.1460-9568.2007.05633.X>
- Cosentino, G., Maiorano, E., Todisco, M., Prunetti, P., Antoniazzi, E., Tammam, G., Quartesan, I., Lettieri, S., De Icco, R., Corsico, A. G., Benazzo, M., Pisani, A., Tassorelli, C., & Alfonsi, E. (2022). Electrophysiological evidence of subclinical trigeminal dysfunction in patients with COVID-19 and smell impairment: A pilot study. *Frontiers in Neurology* , 13 , 2311. <https://doi.org/10.3389/FNEUR.2022.981888/BIBTEX>
- Cruccu, G., Agostino, R., Inghilleri, M., Manfredi, M., & de Visser, B. W. O. (1989). The masseter inhibitory reflex is evoked by innocuous stimuli and mediated by A beta afferent fibres. *Experimental Brain Research* 1989 77:2 , 77 (2), 447–450. <https://doi.org/10.1007/BF00275005>
- Cruccu, G., & Deuschl, G. (2000). The clinical use of brainstem reflexes and hand-muscle reflexes. *Clinical Neurophysiology* , 111 (3), 371–387. [https://doi.org/10.1016/S1388-2457\(99\)00291-6](https://doi.org/10.1016/S1388-2457(99)00291-6)
- Cruccu, G., Iannetti, G. D., Marx, J. J., Thoemke, F., Truini, A., Fitzek, S., Galeotti, F., Urban, P. P., Romaniello, A., Stoeter, P., Manfredi, M., & Hopf, H. C. (2005). Brainstem reflex circuits revisited. *Brain* , 128 (2), 386–394.

- Cruccu, G., Leandri, M., Feliciani, M., & Leandri, M. (1990). Idiopathic and symptomatic trigeminal pain. *Journal of neurology, neurosurgery, and psychiatry* , 53 (12), 1034–1042. <https://doi.org/10.1136/JNRP.53.12.1034>
- Datta, A., Bansal, V., Diaz, J., Patel, J., Reato, D., & Bikson, M. (2009). Gyri-precise head model of transcranial direct current stimulation: Improved spatial focality using a ring electrode versus conventional rectangular pad. *Brain Stimulation* , 2 (4). <https://doi.org/10.1016/j.brs.2009.03.005>
- Datta, A., Bansal, V., Diaz, J., Patel, J., Reato, D., & Bikson, M. (2010). Gyri –precise head model of transcranial DC stimulation. *NIH Public Access* , 2 (4), 201–207. <https://doi.org/10.1016/j.brs.2009.03.005>
- De Visser, B. W. O., Cruccu, G., Manfredi, M., & Koelman, J. H. T. M. (1990). Effects of brainstem lesions on the masseter inhibitory reflex. Functional mechanisms of reflex pathways. *Brain : a journal of neurology* , 113 ( Pt 3) (3), 781–792. <https://doi.org/10.1093/BRAIN/113.3.781>
- De Vito, A., Gastaldo, E., Tugnoli, V., Eleopra, R., Casula, A., Tola, M. R., Granieri, E., & Quatrone, R. (2009). Effect of slow rTMS of motor cortex on the excitability of the blink reflex: A study in healthy humans. *Clinical Neurophysiology: Official Journal of the International Federation of Clinical Neurophysiology* , 120 (1), 174–180. <https://doi.org/10.1016/j.clinph.2008.09.024>
- Optimized multi-electrode stimulation increases focality and intensity at target, 8 *Journal of Neural Engineering* 046011 (2011). <https://doi.org/10.1088/1741-2560/8/4/046011>
- D’Urso, G., Bruzzese, D., Ferrucci, R., Priori, A., Pascotto, A., Galderisi, S., Altamura, A. C., & Bravaccio, C. (2015). Transcranial direct current stimulation for hyperactivity and noncompliance in autistic disorder. *The World Journal of Biological Psychiatry: The Official Journal of the World Federation of Societies of Biological Psychiatry* , 16 (5), 361–366. <https://doi.org/10.3109/15622975.2015.1014411>
- D’Urso, G., Dini, M., Bonato, M., Gallucci, S., Parazzini, M., Maiorana, N., Bortolomasi, M., Priori, A., & Ferrucci, R. (2022). Simultaneous Bilateral Frontal and Bilateral Cerebellar Transcranial Direct Current Stimulation in Treatment-Resistant Depression-Clinical Effects and Electrical Field Modelling of a Novel Electrodes Montage. *Biomedicines* , 10 (7), 1681. <https://doi.org/10.3390/biomedicines10071681>
- Esteban, A. (1999). A neurophysiological approach to brainstem reflexes. Blink reflex. *Neurophysiologie clinique = Clinical neurophysiology* , 29 (1), 7–38. [https://doi.org/10.1016/S0987-7053\(99\)80039-2](https://doi.org/10.1016/S0987-7053(99)80039-2)
- Fearon, C., Lees, A. J., McKinley, J. J., McCarthy, A., Smyth, S., Farrell, M., & Lynch, T. (2021). On the Emergence of Tremor in Prodromal Parkinson’s Disease. *Journal of Parkinson’s Disease* , 11 (1), 261–269. <https://doi.org/10.3233/JPD-202322>
- Ferrucci, R., Bortolomasi, M., Brunoni, A., Vergari, M., Tadini, L., Giacomuzzi, M., & Priori, A. (2009). Comparative benefits of transcranial direct current stimulation (TDCS) treatment in patients with mild/moderate vs. Severe depression. *Clinical Neuropsychiatry* , 6 (6), 246–251.
- Fertonani, A., Rosini, S., Cotelli, M., Rossini, P. M., & Miniussi, C. (2010). Naming facilitation induced by transcranial direct current stimulation. *Behavioural Brain Research* , 208 (2), 311–318. <https://doi.org/10.1016/J.BBR.2009.10.030>
- Fisher, M. A., Shahani, B. T., & Young, R. R. (1979). Assessing segmental excitability after acute rostral lesions: II. The blink reflex. *Neurology* , 29 (1), 45–50. <https://doi.org/10.1212/WNL.29.1.45>
- Francis, J. T., Gluckman, B. J., & Schiff, S. J. (2003). Sensitivity of neurons to weak electric fields. *Journal of Neuroscience* , 23 (19), 7255–7261. <https://doi.org/10.1523/jneurosci.23-19-07255.2003>
- Fritsch, B., Reis, J., Martinowich, K., Schambra, H. M., Ji, Y., Cohen, L. G., & Lu, B. (2010). Direct current stimulation promotes BDNF-dependent synaptic plasticity: Potential implications for motor learning. *Neuron* , 66 (2), 198–204. <https://doi.org/10.1016/j.neuron.2010.03.035>

- Gabriel, C., Gabriel, S., & Corthout, E. (1996). The dielectric properties of biological tissues: I. Literature survey. *Physics in Medicine and Biology* , 41 (11), 2231–2249. Scopus. <https://doi.org/10.1088/0031-9155/41/11/001>
- Gabriel, C., Peyman, A., & Grant, E. H. (2009). Electrical conductivity of tissue at frequencies below 1 MHz. *Physics in Medicine & Biology* , 54 (16), 4863. <https://doi.org/10.1088/0031-9155/54/16/002>
- Gomez-Tames, J., Asai, A., & Hirata, A. (2020). Significant group-level hotspots found in deep brain regions during transcranial direct current stimulation (tDCS): A computational analysis of electric fields. *Clinical Neurophysiology* , 131 (3), 755–765. <https://doi.org/10.1016/j.clinph.2019.11.018>
- Grossman, N., Bono, D., Dedic, N., Kodandaramaiah, S. B., Rudenko, A., Suk, H. J., Cassara, A. M., Neufeld, E., Kuster, N., Tsai, L. H., Pascual-Leone, A., & Boyden, E. S. (2017). Noninvasive Deep Brain Stimulation via Temporally Interfering Electric Fields. *Cell* , 169 (6), 1029-1041.e16. <https://doi.org/10.1016/j.cell.2017.05.024>
- Guidetti, M., Arlotti, M., Bocci, T., Bianchi, A. M., Parazzini, M., Ferrucci, R., & Priori, A. (2022). Electric Fields Induced in the Brain by Transcranial Electric Stimulation: A Review of In Vivo Recordings. *Biomedicines* , 10 (10), Art. 10. <https://doi.org/10.3390/biomedicines10102333>
- Guidetti, M., Bertini, A., Pirone, F., Sala, G., Signorelli, P., Ferrarese, C., Priori, A., & Bocci, T. (2022). Neuroprotection and Non-Invasive Brain Stimulation: Facts or Fiction? *International Journal of Molecular Sciences 2022, Vol. 23, Page 13775* , 23 (22), 13775. <https://doi.org/10.3390/IJMS232213775>
- Guler, S., Dannhauer, M., Erem, B., Macleod, R., Tucker, D., Turovets, S., Luu, P., Erdogmus, D., & Brooks, D. H. (2016). Optimization of focality and direction in dense electrode array transcranial direct current stimulation (tDCS). *Journal of neural engineering* , 13 (3). <https://doi.org/10.1088/1741-2560/13/3/036020>
- Gunalan, K., Howell, B., & McIntyre, C. C. (2018). Quantifying axonal responses in patient-specific models of subthalamic deep brain stimulation. *NeuroImage* , 172 , 263–277. <https://doi.org/10.1016/J.NEUROIMAGE.2018.01.015>
- Holstege, G., Tan, J., van Ham, J. J., & Graveland, G. A. (1986). Anatomical observations on the afferent projections to the retractor bulbi motoneuronal cell group and other pathways possibly related to the blink reflex in the cat. *Brain research* , 374 (2), 321–334. [https://doi.org/10.1016/0006-8993\(86\)90426-9](https://doi.org/10.1016/0006-8993(86)90426-9)
- Huang, Y., Huang, Y., Datta, A., & Parra, L. C. (2020). Optimization of interferential stimulation of the human brain with electrode arrays. *Journal of neural engineering* , 17 (3). <https://doi.org/10.1088/1741-2552/AB92B3>
- Huang, Y., & Parra, L. C. (2019). Can transcranial electric stimulation with multiple electrodes reach deep targets? *Brain Stimulation* , 12 (1), 30–40. <https://doi.org/10.1016/j.brs.2018.09.010>
- Optimized Transcutaneous Spinal Cord Direct Current Stimulation using Multiple Electrodes from 3/9/7 System, 2019 Proceedings of the Annual International Conference of the IEEE Engineering in Medicine and Biology Society, EMBS 6290 (2019). <https://doi.org/10.1109/EMBC.2019.8856689>
- Im, C.-H., Park, J.-H., Shim, M., Chang, W. H., & Kim, Y.-H. (2012). Evaluation of local electric fields generated by transcranial direct current stimulation with an extracephalic reference electrode based on realistic 3D body modeling. *Physics in Medicine & Biology* , 57 (8), 2137. <https://doi.org/10.1088/0031-9155/57/8/2137>
- Kennelly, K. D. (2019). Clinical neurophysiology of cranial nerve disorders. *Handbook of clinical neurology* , 161 , 327–342. <https://doi.org/10.1016/B978-0-444-64142-7.00058-8>
- Khan, A., Antonakakis, M., Vogenauer, N., Haueisen, J., & Wolters, C. H. (2022). Individually optimized multi-channel tDCS for targeting somatosensory cortex. *Clinical Neurophysiology* , 134 , 9–26. <https://doi.org/10.1016/J.CLINPH.2021.10.016>

- Khorrampanah, M., Seyedarabi, H., Daneshvar, S., & Farhoudi, M. (2020). Optimization of montages and electric currents in tDCS. *Computers in Biology and Medicine* , 125 , 103998. <https://doi.org/10.1016/J.COMPBIOMED.2020.103998>
- KIMURA, J. (1973). DISORDER OF INTERNEURONS IN PARKINSONISM: THE ORBICULARIS OCULI REFLEX TO PAIRED STIMULI. *Brain* , 96 (1), 87–96. <https://doi.org/10.1093/brain/96.1.87>
- Kimura, J. (1975). Electrically elicited blink reflex in diagnosis of multiple sclerosis. Review of 260 patients over a seven-year period. *Brain : a journal of neurology* , 98 (3), 413–426. <https://doi.org/10.1093/BRAIN/98.3.413>
- Kimura, J., Daube, J., Burke, D., Hallett, M., Cruccu, G., Ongerboer de Visser, B. W., Yanagisawa, N., Shimamura, M., & Rothwell, J. (1994). Human reflexes and late responses. Report of an IFCN committee. *Electroencephalography and Clinical Neurophysiology* ,90 (6), 393–403. [https://doi.org/10.1016/0013-4694\(94\)90131-7](https://doi.org/10.1016/0013-4694(94)90131-7)
- Kimura, J., & Lyon, L. W. (1972). Orbicularis oculi reflex in the Wallenberg syndrome: Alteration of the late reflex by lesions of the spinal tract and nucleus of the trigeminal nerve. *Journal of neurology, neurosurgery, and psychiatry* , 35 (2), 228–233. <https://doi.org/10.1136/JNPNP.35.2.228>
- Kronberg, G., Rahman, A., Sharma, M., Bikson, M., & Parra, L. C. (2020). Direct current stimulation boosts hebbian plasticity in vitro. *Brain Stimulation: Basic, Translational, and Clinical Research in Neuromodulation* , 13 (2), 287–301. <https://doi.org/10.1016/j.brs.2019.10.014>
- Kugelberg, E. (1952). [Facial reflexes]. *Brain : a journal of neurology* , 75 (3), 385–396. <https://doi.org/10.1093/BRAIN/75.3.385>
- Kuo, H. I., Bikson, M., Datta, A., Minhas, P., Paulus, W., Kuo, M. F., & Nitsche, M. A. (2013). Comparing Cortical Plasticity Induced by Conventional and High-Definition 4 x 1 Ring tDCS: A Neurophysiological Study. *Brain Stimulation* , 6 (4), 644–648. <https://doi.org/10.1016/J.BRS.2012.09.010>
- Kuypers, H. G. J. M. (1958). CORTICOBULBAR CONNEXIONS TO THE PONS AND LOWER BRAIN-STEM IN MANAN ANATOMICAL STUDY. *Brain* , 81 (3), 364–388. <https://doi.org/10.1093/BRAIN/81.3.364>
- Lamy, J.-C., & Boakye, M. (2013). BDNF Val66Met polymorphism alters spinal DC stimulation-induced plasticity in humans. *Journal of Neurophysiology* , 110 (1), 109–116. <https://doi.org/10.1152/jn.00116.2013>
- Lang, N., Siebner, H. R., Chadaide, Z., Boros, K., Nitsche, M. A., Rothwell, J. C., Paulus, W., & Antal, A. (2007). Bidirectional Modulation of Primary Visual Cortex Excitability: A Combined tDCS and rTMS Study. *Investigative Ophthalmology & Visual Science* ,48 (12), 5782–5787. <https://doi.org/10.1167/IOVS.07-0706>
- Evidence-based guidelines on the therapeutic use of transcranial direct current stimulation (tDCS), 128 *Clinical Neurophysiology* 56 (2017). <https://doi.org/10.1016/j.clinph.2016.10.087>
- Manca, D., Muoz, E., Pastor, P., Valldeoriola, F., & Valls-Sole, J. (2001). Enhanced gain of blink reflex responses to ipsilateral supraorbital nerve afferent inputs in patients with facial nerve palsy. *Clinical Neurophysiology* , 112 (1), 153–156. [https://doi.org/10.1016/S1388-2457\(00\)00516-2](https://doi.org/10.1016/S1388-2457(00)00516-2)
- Manto, M., Argyropoulos, G. P. D., Bocci, T., Celnik, P. A., Corben, L. A., Guidetti, M., Koch, G., Priori, A., Rothwell, J. C., Sadnicka, A., Spampinato, D., Ugawa, Y., Wessel, M. J., & Ferrucci, R. (2021). Consensus Paper: Novel Directions and Next Steps of Non-invasive Brain Stimulation of the Cerebellum in Health and Disease. *Cerebellum (London, England)* . <https://doi.org/10.1007/s12311-021-01344-6>
- Mao, J. B., & Evinger, C. (2001). Long-Term Potentiation of the Human Blink Reflex. *Journal of Neuroscience* , 21 (12), RC151–RC151. <https://doi.org/10.1523/JNEUROSCI.21-12-J0002.2001>

- Marceglia, S., Guidetti, M., Harmsen, I. E., Loh, A., Meoni, S., Foffani, G., Lozano, A. M., Volkmann, J., Moro, E., & Priori, A. (2021). Deep brain stimulation: Is it time to change gears by closing the loop? *Journal of Neural Engineering* , 18 (6). <https://doi.org/10.1088/1741-2552/ac3267>
- Mendonca, M. E., Santana, M. B., Baptista, A. F., Datta, A., Bikson, M., Fregni, F., & Araujo, C. P. (2011). Transcranial DC Stimulation in Fibromyalgia: Optimized Cortical Target Supported by High-Resolution Computational Models. *The Journal of Pain* , 12 (5), 610–617. <https://doi.org/10.1016/J.JPAIN.2010.12.015>
- Mesquita, P. H. C., Franchini, E., Romano-Silva, M. A., Lage, G. M., & Albuquerque, M. R. (2020). Transcranial Direct Current Stimulation: No Effect on Aerobic Performance, Heart Rate, or Rating of Perceived Exertion in a Progressive Taekwondo-Specific Test. *International Journal of Sports Physiology and Performance* , 15 (7), 958–963. <https://doi.org/10.1123/IJSPP.2019-0410>
- Mishra, P., Pandey, C. M., Singh, U., Gupta, A., Sahu, C., & Keshri, A. (2019). Descriptive Statistics and Normality Tests for Statistical Data. *Annals of Cardiac Anaesthesia* , 22 (1), 67. <https://doi.org/10.4103/ACA.ACA.157.18>
- Transcranial direct current stimulation: State of the art 2008* , 1 206 (2008) (testimony of Michael A. Nitsche, Leonardo G. Cohen, Eric M. Wassermann, Alberto Priori, Nicolas Lang, Andrea Antal, Walter Paulus, Friedhelm Hummel, Paulo S. Boggio, Felipe Fregni, Alvaro Pascual-Leone, Nitsche MA, Cohen LG, Wassermann EM, Pascual-Leone Priori A, Lang N, Antal A, Paulus W, Hummel F, . . . Pascual-Leone Priori A).
- Nitsche, M. A., & Paulus, W. (2000). Excitability changes induced in the human motor cortex by weak transcranial direct current stimulation. *Journal of Physiology* , 527 (3), 633–639. <https://doi.org/10.1111/j.1469-7793.2000.t01-1-00633.x>
- Noetscher, G. M., Yanamadala, J., Makarov, S. N., & Pascual-Leone, A. (2014). Comparison of cephalic and extracephalic montages for transcranial direct current stimulation—a numerical study. *IEEE Transactions on Biomedical Engineering* , 61 (9), 2488–2498. <https://doi.org/10.1109/TBME.2014.2322774>
- Nonnekes, J., Arroggi, A., Munneke, M. A. M., Van Asseldonk, E. H. F., Nijhuis, L. B. O., Geurts, A. C., & Weerdesteyn, V. (2014). Subcortical Structures in Humans Can Be Facilitated by Transcranial Direct Current Stimulation. *PLOS ONE* , 9 (9), e107731. <https://doi.org/10.1371/JOURNAL.PONE.0107731>
- Ongerboer De Visser, B. W., & Goor, C. (1976). Jaw reflexes and masseter electromyograms in mesencephalic and pontine lesions: An electrodiagnostic study. *Journal of neurology, neurosurgery, and psychiatry* , 39 (1), 90–92. <https://doi.org/10.1136/JNPN.39.1.90>
- Ongerboer De Visser, B. W., & Kuypers, H. G. J. M. (1978). Late blink reflex changes in lateral medullary lesions. An electrophysiological and neuro-anatomical study of Wallenberg's Syndrome. *Brain : a journal of neurology* , 101 (2), 285–294. <https://doi.org/10.1093/BRAIN/101.2.285>
- Opitz, A., Paulus, W., Will, S., Antunes, A., & Thielscher, A. (2015). Determinants of the electric field during transcranial direct current stimulation. *NeuroImage* , 109 , 140–150. <https://doi.org/10.1016/j.neuroimage.2015.01.033>
- Parazzini, M., Fiocchi, S., & Ravazzani, P. (2012). Electric field and current density distribution in an anatomical head model during transcranial direct current stimulation for tinnitus treatment. *Bioelectromagnetics* , 33 (6), 476–487.
- Parazzini, M., Fiocchi, S., Rossi, E., Paglialonga, A., & Ravazzani, P. (2011). Transcranial direct current stimulation: Estimation of the electric field and of the current density in an anatomical human head model. *IEEE Transactions on Biomedical Engineering* , 58 (6), 1773–1780. <https://doi.org/10.1109/TBME.2011.2116019>

- Parazzini, M., Rossi, E., Ferrucci, R., Liorni, I., Priori, A., & Ravazzani, P. (2014). Modelling the electric field and the current density generated by cerebellar transcranial DC stimulation in humans. *Clinical Neurophysiology* , 125 (3), 577–584. <https://doi.org/10.1016/j.clinph.2013.09.039>
- Parazzini, M., Rossi, E., Rossi, L., Priori, A., Ravazzani, P., Cogiamanian, F., Marceglia, S., Ardolino, G., Barbieri, S., & Priori, A. (2013). Evaluation of the current density in the brainstem during transcranial direct current stimulation with extra-cephalic reference electrode. *Clinical Neurophysiology* , 124 (5), 1039–1040. <https://doi.org/10.1016/J.CLINPH.2012.09.021>
- Park, J. H., Hong, S. B., Kim, D. W., Suh, M., & Im, C. H. (2011). A novel array-type transcranial direct current stimulation (tDCS) system for accurate focusing on targeted brain areas. *IEEE Transactions on Magnetics* , 47 (5), 882–885. <https://doi.org/10.1109/TMAG.2010.2072987>
- Pellegrini, M., Zoghi, M., & Jaberzadeh, S. (2021). The effects of transcranial direct current stimulation on corticospinal and cortico-cortical excitability and response variability: Conventional versus high-definition montages. *Neuroscience Research* , 166 , 12–25. <https://doi.org/10.1016/j.neures.2020.06.002>
- Peterchev, A. V., Wagner, T. A., Miranda, P. C., Nitsche, M. A., Paulus, W., Lisanby, S. H., Pascual-Leone, A., & Bikson, M. (2012). Fundamentals of transcranial electric and magnetic stimulation dose: Definition, selection, and reporting practices. *Brain Stimulation* , 5 (4), 435–453. <https://doi.org/10.1016/j.brs.2011.10.001>
- Priori, A., Berardelli, A., Rona, S., Accornero, N., Manfredi, M., A, P., A, B., S, R., N, A., & M, M. (1998). *Polarization of the human motor cortex through the scalp* . 9 (10), 2257–2260. <https://doi.org/10.1097/00001756-199807130-00020>
- Priori, A., Maiorana, N., Dini, M., Guidetti, M., Marceglia, S., & Ferrucci, R. (2021). Adaptive deep brain stimulation (aDBS). *International Review of Neurobiology* , 159 , 111–127. <https://doi.org/10.1016/bs.irm.2021.06.006>
- Rashed, E. A., Gomez-Tames, J., & Hirata, A. (2020). End-to-end semantic segmentation of personalized deep brain structures for non-invasive brain stimulation. *Neural Networks* , 125 , 233–244. <https://doi.org/10.1016/j.neunet.2020.02.006>
- Reato, D., Rahman, A., Bikson, M., & Parra, L. C. (2010). Low-intensity electrical stimulation affects network dynamics by modulating population rate and spike timing. *The Journal of neuroscience : the official journal of the Society for Neuroscience* , 30 (45), 15067–15079. <https://doi.org/10.1523/JNEUROSCI.2059-10.2010>
- Roos, D., Biermann, L., Jarczok, T. A., & Bender, S. (2021). Local Differences in Cortical Excitability – A Systematic Mapping Study of the TMS-Evoked N100 Component. *Frontiers in Neuroscience* , 15 . <https://www.frontiersin.org/articles/10.3389/fnins.2021.623692>
- Ruffini, G., Fox, M. D., Ripolles, O., Miranda, P. C., & Pascual-Leone, A. (2014). Optimization of multifocal transcranial current stimulation for weighted cortical pattern targeting from realistic modeling of electric fields. *NeuroImage* , 89 , 216–225. <https://doi.org/10.1016/J.NEUROIMAGE.2013.12.002>
- Sadleir, R. J., Vannorsdall, T. D., Schretlen, D. J., & Gordon, B. (2012). Target optimization in transcranial direct current stimulation. *Frontiers in Psychiatry* , 3 (OCT), 90. <https://doi.org/10.3389/FPSYT.2012.00090/BIBTEX>
- Schoenen, J. (1993). Exteroceptive suppression of temporalis muscle activity: Methodological and physiological aspects. *Cephalalgia : an international journal of headache* , 13 (1), 3–10. <https://doi.org/10.1046/J.1468-2982.1993.1301003.X>
- Shahani, B. T., & Young, R. R. (1972). Human orbicularis oculi reflexes. *Neurology* , 22 (2), 149–154. <https://doi.org/10.1212/WNL.22.2.149>

- Siebner, H. R., Lang, N., Rizzo, V., Nitsche, M. A., Paulus, W., Lemon, R. N., & Rothwell, J. C. (2004). Preconditioning of Low-Frequency Repetitive Transcranial Magnetic Stimulation with Transcranial Direct Current Stimulation: Evidence for Homeostatic Plasticity in the Human Motor Cortex. *Journal of Neuroscience* , 24 (13), 3379–3385. <https://doi.org/10.1523/JNEUROSCI.5316-03.2004>
- Thomas, C., Huang, Y., Faria, P. C., & Datta, A. (2019). High-resolution head model of transcranial direct current stimulation: A labeling analysis. *Proceedings of the Annual International Conference of the IEEE Engineering in Medicine and Biology Society, EMBS* , 6442–6445. <https://doi.org/10.1109/EMBC.2019.8857181>
- Wagner, S., Burger, M., & Wolters, C. H. (2016). An optimization approach for well-targeted transcranial direct current stimulation. *SIAM Journal on Applied Mathematics* , 76 (6), 2154–2174. <https://doi.org/10.1137/15M1026481>
- Woods, A. J., Antal, A., Bikson, M., Boggio, P. S., Brunoni, A. R., Celnik, P., Cohen, L. G., Fregni, F., Herrmann, C. S., Kappenman, E. S., Knotkova, H., Liebetanz, D., Miniussi, C., Miranda, P. C., Paulus, W., Priori, A., Reato, D., Stagg, C., Wenderoth, N., & Nitsche, M. A. (2016). A technical guide to tDCS, and related non-invasive brain stimulation tools. *Clinical Neurophysiology* , 127 (2), 1031–1048. <https://doi.org/10.1016/j.clinph.2015.11.012>



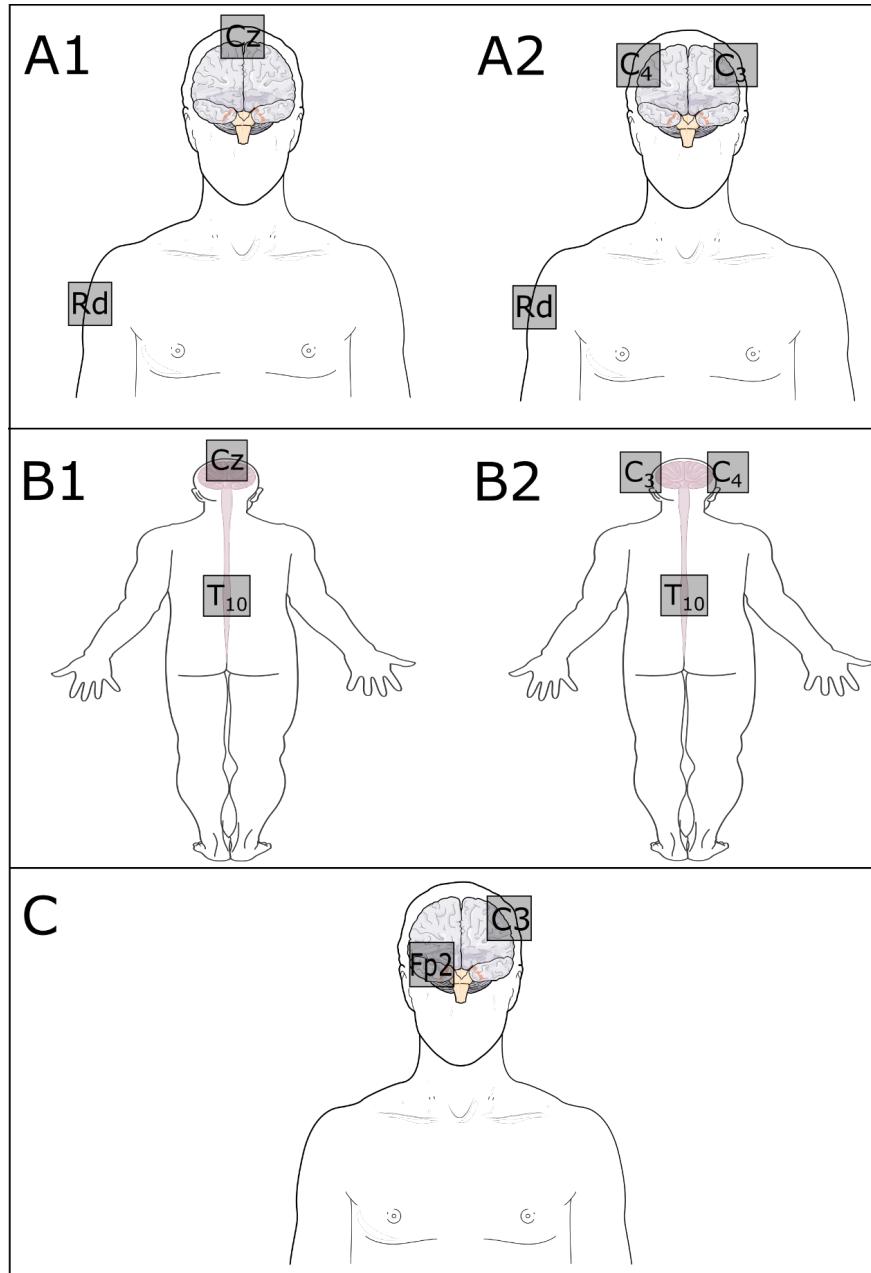


**Fig. 1. tDCS montages for computational models. A1)** Active electrode: Cz, return electrode: right deltoid; **A2)** Active electrodes: C3, C4, return electrode: right deltoid; **B1)** Active electrode: Cz, return electrode: T10; **B2)** Active electrodes: C3, C4, return electrode: T10; **C)** Active electrode: C3, Return electrode: Fp2.

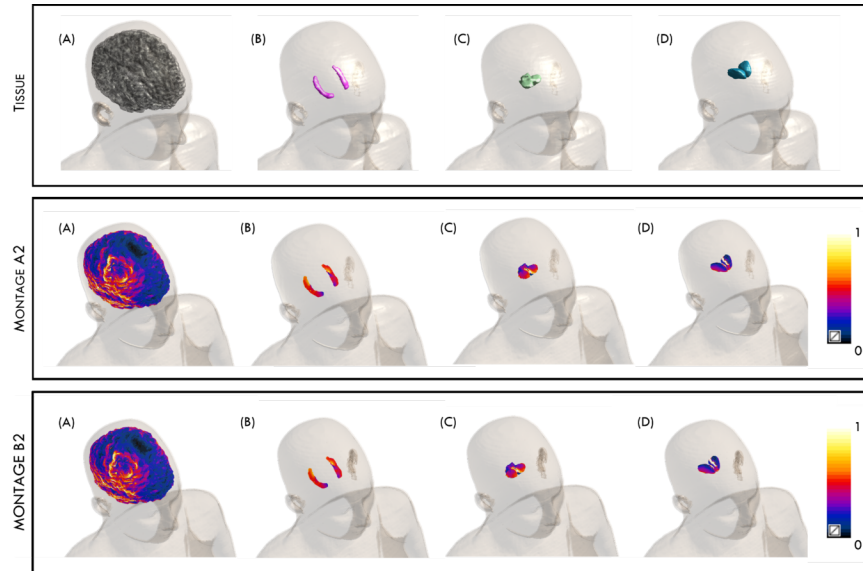


**Fig. 2. First row:** the 4 different brain structures considered as region of interest (ROIs) - grey matter (A), hippocampus (B), mid-brain (C), and thalamus (D). **Second row:** the view of the estimated EF amplitude distribution over grey matter (A), hippocampus (B), midbrain (C), and thalamus (D) for montage A2 (active electrodes over C3, C4; return electrode over right deltoid). **Third row:** view of the estimated EF amplitude distribution over grey matter (A), hippocampus (B), mid-brain (C), and thalamus (D) for montage B2 (active electrodes over C3, C4; return electrode over the spinal process of the tenth thoracic vertebra). The values are normalized with respect to the 99th percentile in grey matter.

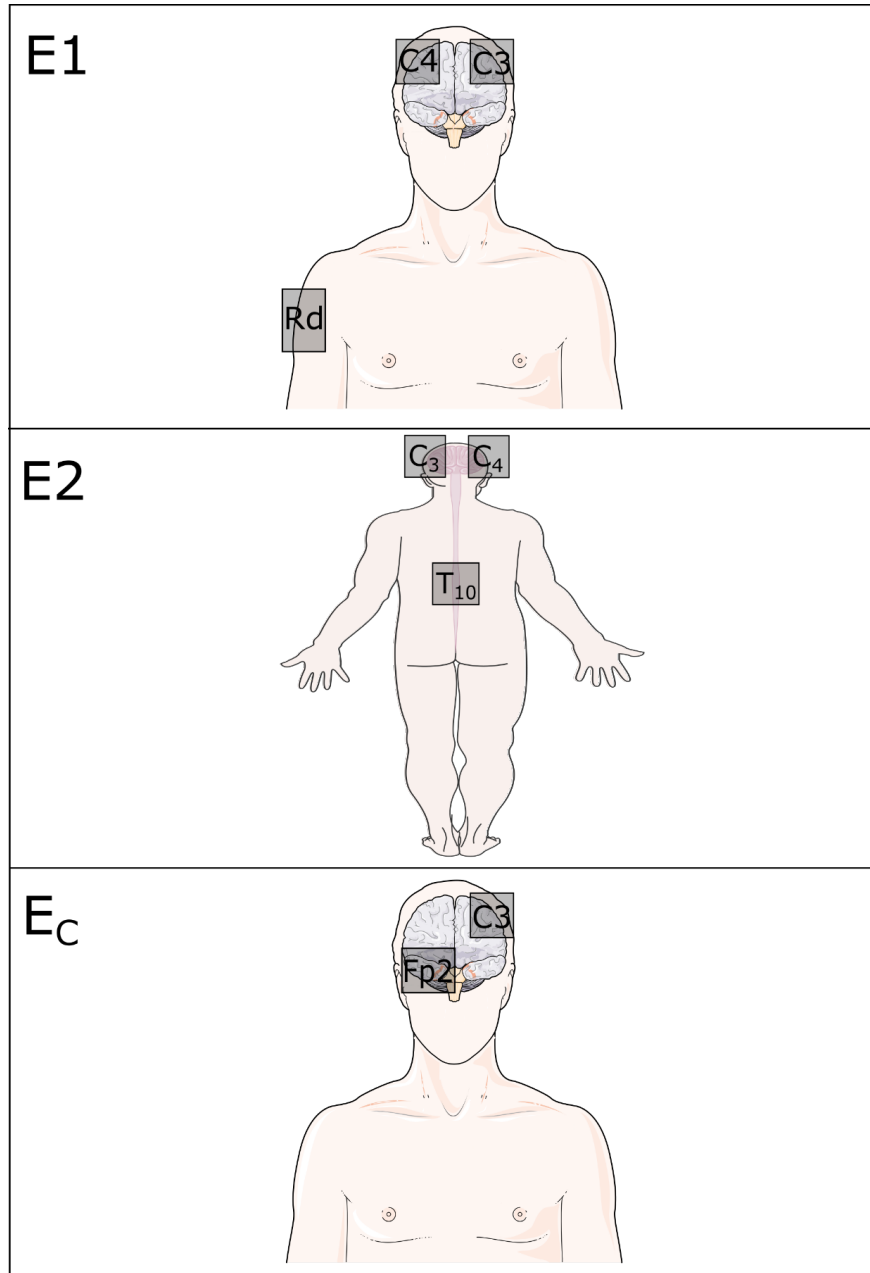


**Fig. 3. tDCS montages for clinical experiments. E1)** Anodes: C3, C4; Cathode: right deltoid; **E2)** Anodes: C3, C4; Cathode: T10; **C)** Anode: C3; Cathode: Fp2.

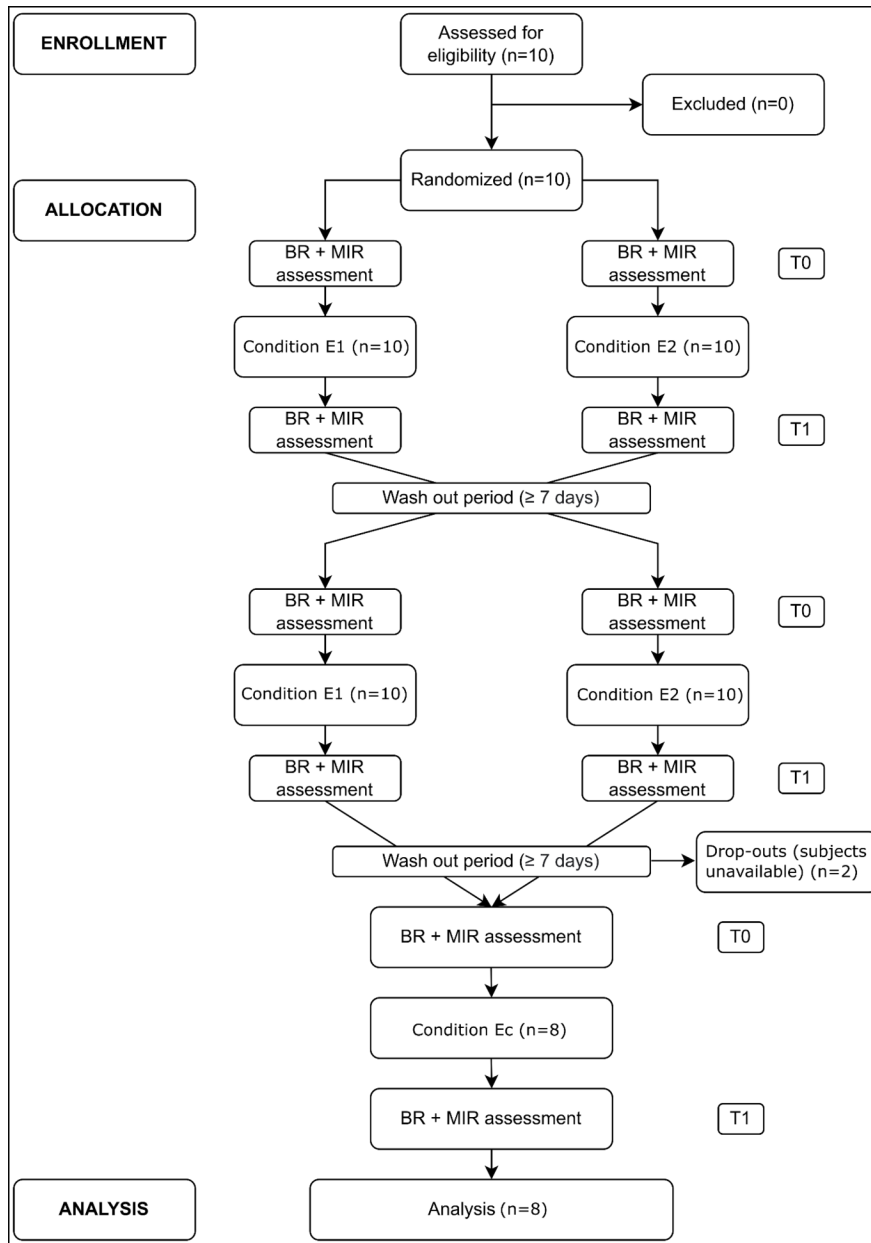


**Fig. 4.** Flowchart diagram depicting the flow of participants through study.

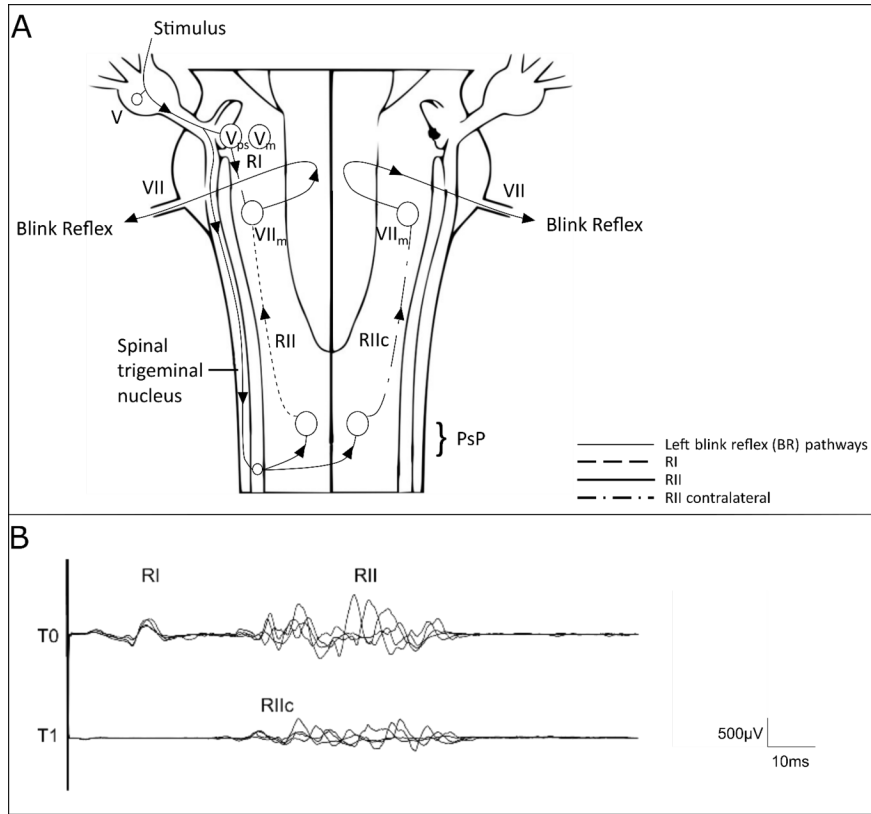


**Fig.5. Blink Reflex pathways (Left BR).** Image represents the relation between BR traces and the presumed locations of bulbar interneurons subserving the two main components of BR, RI and RII (ipsilateral and contralateral). **A** . Schematic representation of the brainstem circuits of the BR. **B** . Electrophysiological traces corresponding to brainstem circuits as recorded by left and right orbicularis oculi muscle (patient's age = 55; Stimulation intensity set at 14.5 mA). V = trigeminal nerve; V<sub>ps</sub> = principal sensory trigeminal nucleus; V<sub>m</sub> = motor nucleus of trigeminal nerve; VII<sub>m</sub> = motor nucleus of facial nerve; PsP = polysynaptic pathways; RIIc = RII contralateral.

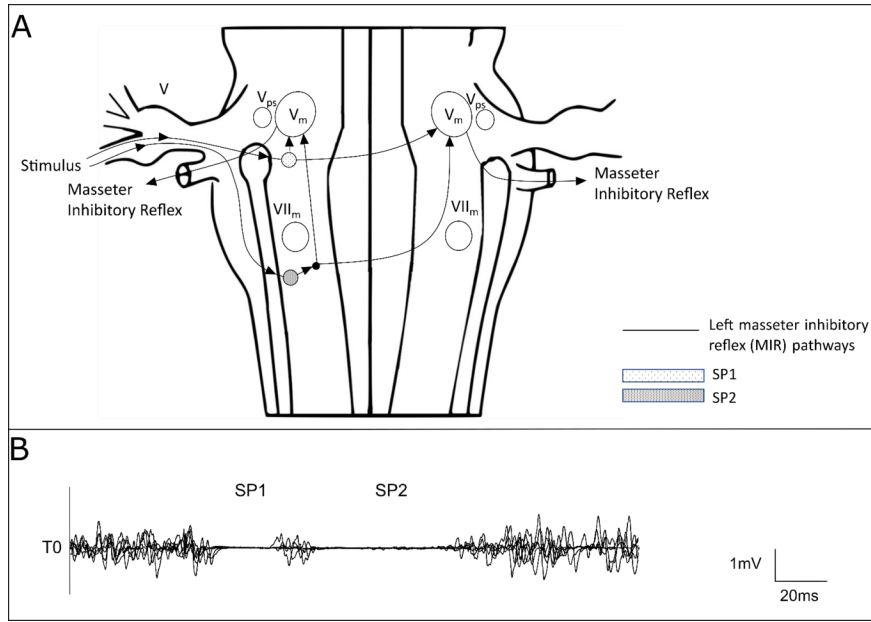


**Fig.6. Masseter Inhibitory Reflex pathways (Left MIR).** Image represents the relation between MIR traces and presumed locations of bulbar interneurons subserving the early (SP1) and late (SP2) phase of MIR. **A** . Schematic representation of the brainstem circuits of the MIR. **B** . Electrophysiological traces corresponding to brainstem circuits as recorded by left and right masseter muscle (patient's age = 25; Stimulation intensity set at 42 mA). V = trigeminal nerve; V<sub>ps</sub> = principal sensory trigeminal nucleus; V<sub>m</sub> = motor nucleus of trigeminal nerve; VII<sub>m</sub> = motor nucleus of facial nerve.

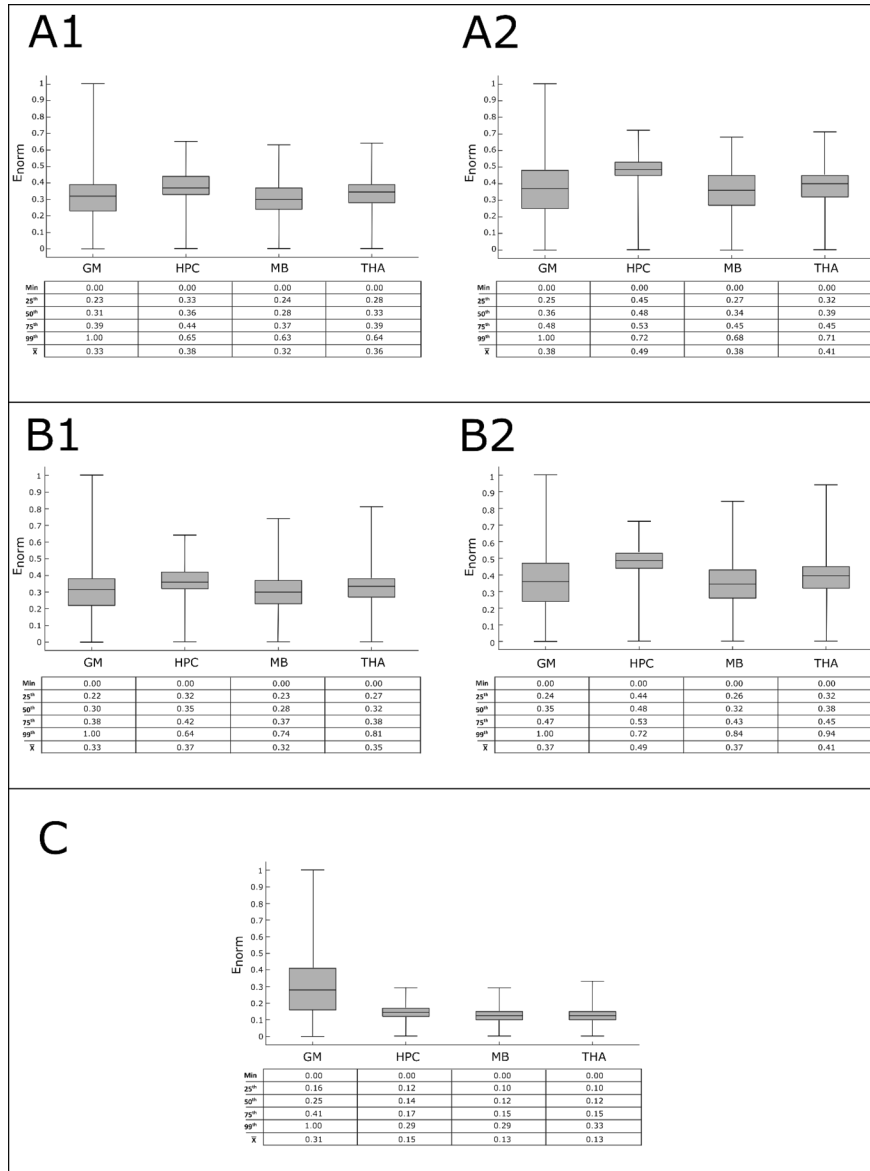


**Fig. 7. Quantitative distributions of E in the grey matter (GM), hippocampus (HPC), mid-brain (MB), and thalamus (THA) for montages (A1, B2, B1, B2, C) in the computational models. The values (minimum, 25<sup>th</sup> percentile, median, 75<sup>th</sup> percentile, 99<sup>th</sup> percentile, mean) are displayed with respect to the 99<sup>th</sup> percentile in grey matter.**

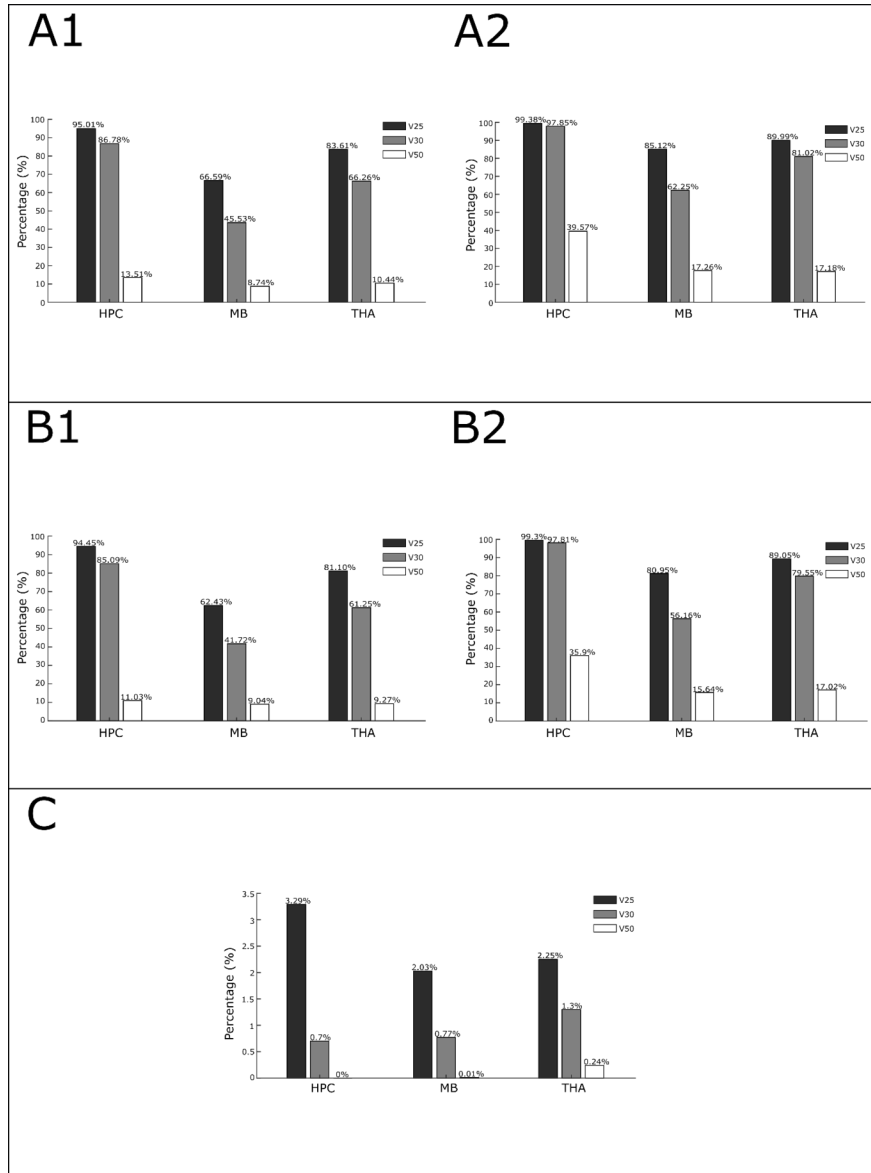


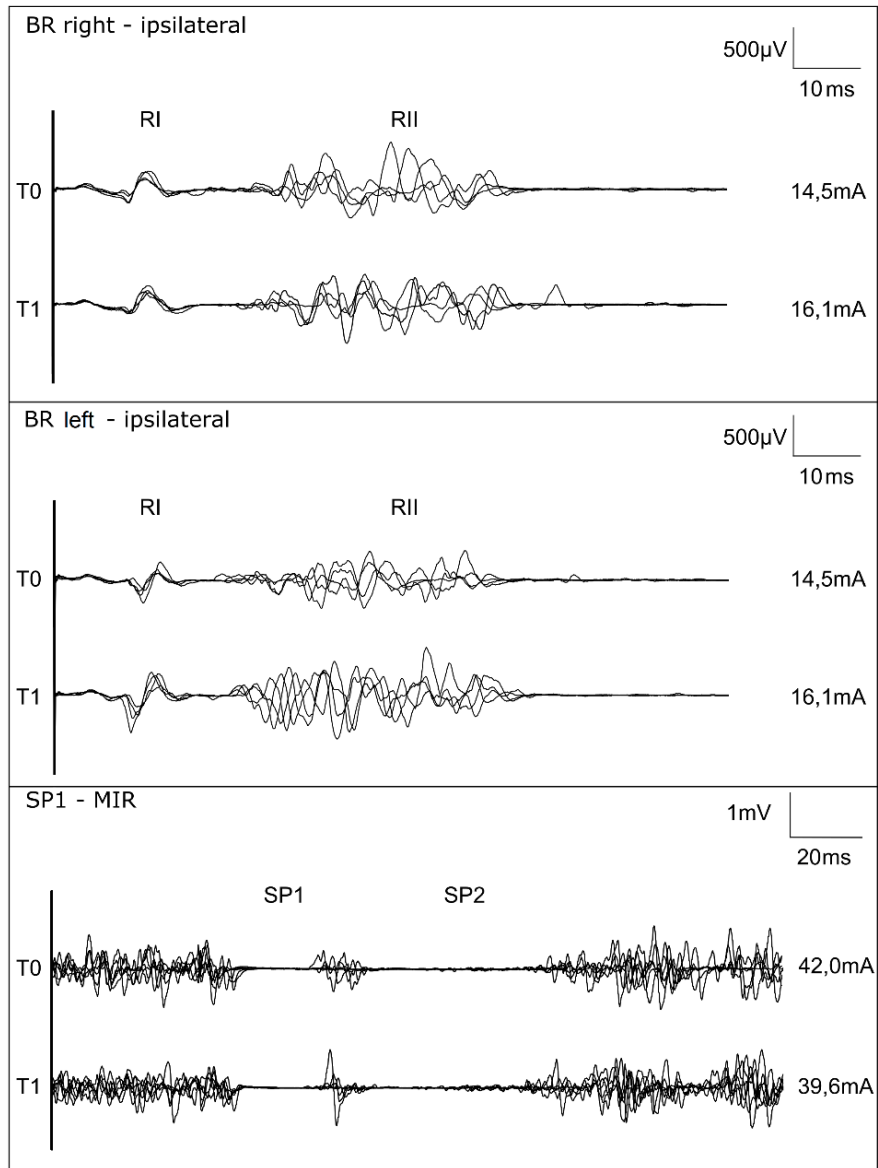
**Fig.8. V25, V30 and V50 of hippocampus (HPC), midbrain (MB) and thalamus (THA) for montages (A1, B2, B1, B2, C) in the computational models . The values are displayed with respect to the 99th percentile in grey matter.**

**Table 1. Neurophysiological assessments.** Characteristics of blink reflex (threshold, RI latency, RII latency ipsilateral, RII latency contralateral) and masseter inhibitory reflex (threshold, latency SP1, duration SP1, latency SP2, duration SP2) are reported at T0 and T1, according to the treatment condition (A, B, or C) group (anodal or sham tsDCS). Values are expressed mean values  $\pm$  standard error (S.E.), p refers to Paired Sample T-Test.

	Condition E1	Condition E1		Condition E2	Condition E2	
	T0	T1	p	T0	T1	p
<b>Blink Reflex (R)</b>						



	Condition E1	Condition E1		Condition E2	Condition E2	
Threshold	17.47 ± 2.19	18.52 ± 2	0.76	17.33 ± 2.19	17.15 ± 2.05	0.90
RI latency	10.6 ± 0.22	9.89 ± 0.23	<b>&lt;0.001</b>	10.21 ± 0.21	9.87 ± 0.13	0.09
RII latency ipsilateral	30.53 ± 1.28	31.57 ± 1.39	0.052	30.54 ± 1.26	29.60 ± 0.80	0.26
RII latency contralateral	31.01 ± 1.36	32.05 ± 1.51	0.054	31.09 ± 1.15	31.07 ± 0.81	0.97
<b>Blink Reflex (L)</b>						
Threshold	17.56 ± 2.11	18.41 ± 1.8	0.66	17.22 ± 1.94	18.06 ± 1.84	0.64
RI latency	10.57 ± 0.27	10.08 ± 0.22	<b>0.01</b>	10.23 ± 0.22	9.80 ± 0.23	0.08
RII latency ipsilateral	30.1 ± 1.41	30.3 ± 1.08	0.84	30.45 ± 1.33	28.36 ± 0.72	0.09
RII latency contralateral	31.29 ± 1.70	32.24 ± 1.18	0.46	31.73 ± 1.10	29.98 ± 0.70	0.11
<b>Masseter Inhibitory Reflex</b>						
Threshold	18.3 ± 1.38	18.34 ± 1.35	0.97	18.48 ± 0.92	17.78 ± 1.23	0.47
Latency SP1	14.33 ± 0.65	14.06 ± 0.50	0.56	13.65 ± 0.79	12.93 ± 0.62	0.15
Duration SP1	13.12 ± 1.03	17.06 ± 2.31	<b>0.03</b>	13.66 ± 1.45	16.55 ± 1.80	0.17
Latency SP2	49.99 ± 2.51	49.06 ± 2.43	0.77	50.67 ± 3.4	49.63 ± 2.54	0.46
Duration SP2	29.84 ± 3.14	29.31 ± 2.97	0.84	31.39 ± 5.57	28.8 ± 4.15	0.46



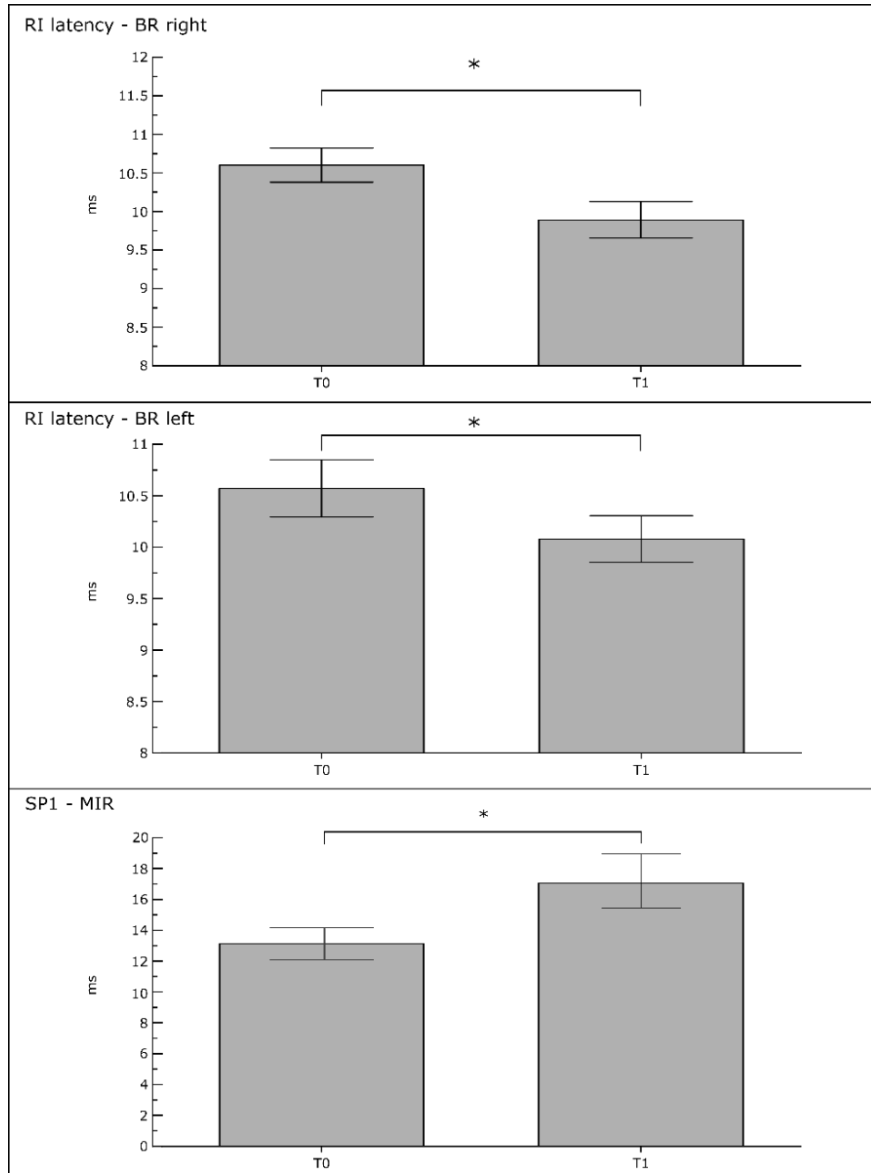


**Fig.9. Neurophysiological changes in condition E1. Left.** Exemplificative averaged traces of BR (R), BR (L) (patient's age = 55), and MIR (patient's age = 25) recorded before (T0) and after (T1). Side values refer to stimulation intensities. **Right .** Changes in R1 latency (BR left), R1 latency (BR right), and SP1 (MIR) (\* $p < 0.05$ , Paired Sample T-Test).

#### Hosted file

Fig.1.docx available at <https://authorea.com/users/593343/articles/628407-monopolar-transcranial-direct-current-stimulation-tcds-might-selectively-affect-brainstem-reflex-pathways-a-computational-and-neurophysiological-study>

#### Hosted file

Fig.2.docx available at <https://authorea.com/users/593343/articles/628407-monopolar-transcranial-direct-current-stimulation-tcds-might-selectively-affect-brainstem-reflex-pathways-a-computational-and-neurophysiological-study>

[pathways-a-computational-and-neurophysiological-study](#)

**Hosted file**

Fig.3.docx available at <https://authorea.com/users/593343/articles/628407-monopolar-transcranial-direct-current-stimulation-tdcs-might-selectively-affect-brainstem-reflex-pathways-a-computational-and-neurophysiological-study>

**Hosted file**

Fig.4.docx available at <https://authorea.com/users/593343/articles/628407-monopolar-transcranial-direct-current-stimulation-tdcs-might-selectively-affect-brainstem-reflex-pathways-a-computational-and-neurophysiological-study>

**Hosted file**

Fig.5.docx available at <https://authorea.com/users/593343/articles/628407-monopolar-transcranial-direct-current-stimulation-tdcs-might-selectively-affect-brainstem-reflex-pathways-a-computational-and-neurophysiological-study>

**Hosted file**

Fig.6.docx available at <https://authorea.com/users/593343/articles/628407-monopolar-transcranial-direct-current-stimulation-tdcs-might-selectively-affect-brainstem-reflex-pathways-a-computational-and-neurophysiological-study>

**Hosted file**

Fig.7.docx available at <https://authorea.com/users/593343/articles/628407-monopolar-transcranial-direct-current-stimulation-tdcs-might-selectively-affect-brainstem-reflex-pathways-a-computational-and-neurophysiological-study>

**Hosted file**

Fig.8.docx available at <https://authorea.com/users/593343/articles/628407-monopolar-transcranial-direct-current-stimulation-tdcs-might-selectively-affect-brainstem-reflex-pathways-a-computational-and-neurophysiological-study>

**Hosted file**

Table 1.docx available at <https://authorea.com/users/593343/articles/628407-monopolar-transcranial-direct-current-stimulation-tdcs-might-selectively-affect-brainstem-reflex-pathways-a-computational-and-neurophysiological-study>

**Hosted file**

Fig.9.docx available at <https://authorea.com/users/593343/articles/628407-monopolar-transcranial-direct-current-stimulation-tdcs-might-selectively-affect-brainstem-reflex-pathways-a-computational-and-neurophysiological-study>